ACADEMIC PRESS

Available online at www.sciencedirect.com

SCIENCE DIRECT

Journal of Sound and Vibration 264 (2003) 893–910

JOURNAL OF SOUND AND VIBRATION

www.elsevier.com/locate/jsvi

Vibration and damping analysis of annular plates with constrained damping layer treatments

Horng-Jou Wang, Lien-Wen Chen*

Department of Mechanical Engineering, National Cheng Kung University, Tainan 70101, Taiwan

Received 21 February 2002; accepted 5 August 2002

Abstract

The natural frequencies and modal loss factors of annular plates with fully and partially constrained damping treatments are considered. The equations of free vibration of the plate including the transverse shear effects are derived by a discrete layer annular finite element method. The extensional and shear moduli of the viscoelastic material layer are described by the complex quantities. Complex eigenvalues are then found numerically, and from these, both frequencies and loss factors are extracted. The effects of viscoelastic layer stiffness and thickness, constraining layer stiffness and thickness, and treatment size on natural frequencies and modal loss factors are presented. Numerical results also show that the longer constrained damping treatment in radial length does not always provide better damping than the shorter ones.

1. Introduction

One of the approaches to solve certain resonant noise and vibration problems is the surface damping treatment. The treatments can easily be applied to existing structures and provide high damping capability over wide temperature and frequency ranges. The major damping mechanism in vibrations is due to the extensional or shear deformation of the viscoelastic materials [1]. The extensional damping treatment, sometimes called the unconstrained damping treatment, is coated on one or both sides of a structure, so that whenever the structure is subjected to the cyclic bending, the damping material will be subjected to tension–compression deformations. The shear type of damping treatment is similar to the extensional type, except that the viscoelastic material is

*Corresponding author. Tel.: +886-6-275-7575 ext. 62143; fax: +886-6-235-2973.
E-mail address: chenlw@mail.ncku.edu.tw (L.-W. Chen).

0022-460X/03/$ - see front matter
doi:10.1016/S0022-460X(02)01232-4

constrained by a much stiffer elastic layer, usually metallic. Whenever the treatment is subjected to cyclic bending, the metal layer will constrain the viscoelastic material and force it to deform in shear. This type of treatment is also referred to as the constrained damping treatment. For a given weight, Mead [2] showed that the shear type of damping treatment is more efficient than the extensional one.

Numerous investigations on the vibration and damping properties of basic structures, such as beams and rectangular plates, with fully constrained damping layer treatments are available. Kerwin [3] discussed the problem first. Ross, Ungar and Kerwin (RKU) [4] presented a fourth order theory to predict damping in plates with constrained layer treatments. DiTaranto [5] derived the sixth order theory for constrained layer damped beams with arbitrary boundary conditions, and Mead and Markus [6] refined the theory of DiTaranto. The governing equations of flexural vibration of a symmetrical sandwich rectangular plate were presented by Mead [7]. Rao and Nakra [8] proposed a set of 12th order partial differential governing equations including bending–extension coupling of unsymmetrical sandwich plates. Non-symmetric layouts were discussed by He and Ma [9] via the modal strain energy method. The effects of shear deformation and rotational inertia of damped structures have also been taken into account in many references. Rao [10] studied the vibration of short sandwich beams. Rikards et al. [11] studied the vibration and damping of laminated composite beams by using a simple Timoshenko beam finite element. Cupial and Niziol [12] considered a three-layered rectangular plate with a viscoelastic core layer and laminated face layers by the first order shear deformation theory. Zapfe and Lesieutre [13] investigated the dynamic analysis of composite sandwich beams with integral damping layers by a discrete layer beam finite element.

Circular plates are widely used in mechanical applications, and vibrations of circular plates have been discussed for many decades. However, the studies of constrained damping layer treatment to circular plates were few, and all focused on the fully constrained damping treatment. Mirza and Singh [14] studied the axisymmetric vibration of a circular sandwich plate. Roy and Ganesan [15] developed a finite element method for vibration and damping analyses of circular plates with the constrained damping layer treatment. The situations when the viscoelastic material core layer is thicker than the face layers were considered in both of these papers. Yu and Huang [16] derived the equations of motion of a three-layer circular plate based on the thin shell theory to handle the very thin viscoelastic layer problem, but only the iso-symmetric annular plate solutions were obtained.

In practice, the constraining layer and the host plate are not always of the same material or of identical thickness, and the additional damping layer and the constraining layer are thinner than the host plate. Also, partial damping treatment is necessary because of material, thermal, packaging, weight or cost constraints. The present paper will study the vibration behavior of an annular plate with fully and partially constrained damping treatment. The discrete layer annular finite elements including transverse shear effects are adopted, and the extensional and shear moduli of the viscoelastic material layer are described by the complex quantities. By solving the complex eigenvalue problem, the natural frequencies and modal loss factors of the composite plate are obtained. The effects of the design parameters of the treatment, such as damping layer stiffness and thickness, constraining layer stiffness and thickness, and treatment size are discussed.

2. Finite element formulation

The structure of interest is indicated in Fig. 1, the annular plate of inner radius a and outer radius b is partially treated with a constrained damping layer. The annular constrained damping layer covering has an inner radius a' and outer radius b' and is composed of two layers: layer 3 is a pure elastic, isotropic and homogeneous constraining layer and layer 2 is the linear viscoelastic material layer. Layer 2 is an adhesive capable of dissipating vibratory motions. The host annular plate is assumed to be undamped, isotropic and homogeneous and is designated as layer 1. The thicknesses of the three layers are h_1, h_2, and h_3, respectively.

The discrete layer annular finite element [15] is adopted, as shown in Fig. 2(a). The annular element of inner radius r_i and outer radius r_o for layer i has 12 degrees of freedom. These are the displacements in the r direction—U_i^A, U_{i+1}^A, U_i^B and U_{i+1}^B, the displacements in the θ direction—V_i^A, V_{i+1}^A, V_i^B and V_{i+1}^B, the transverse displacements—W^A and W^B, and the rotation angles—Θ^A, and Θ^B. Under the assumption that the transverse displacements are constant through the thickness of the plate, i.e., the transverse normal strain is zero, the nodal degrees of freedom for three-layer discrete layer annular finite elements are shown in Fig. 2(b).

The displacement field of the ith layer, $\mathbf{u}_i = \{ u_i \quad v_i \quad w_i \}^{\mathrm{T}}$, can be expressed in terms of the in-plane displacements of the adjacent layer interfaces and the transverse displacement, $\{ U_i \quad V_i \quad U_{i+1} \quad V_{i+1} \quad W \}^{\mathrm{T}}$, as

$$\begin{Bmatrix} u_i(r,\theta,z,t) \\ v_i(r,\theta,z,t) \\ w_i(r,\theta,t) \end{Bmatrix} = \mathbf{L}_{1,i}(z) \begin{Bmatrix} U_i(r,\theta,t) \\ V_i(r,\theta,t) \\ U_{i+1}(r,\theta,t) \\ V_{i+1}(r,\theta,t) \\ W(r,\theta,t) \end{Bmatrix}, \tag{1}$$

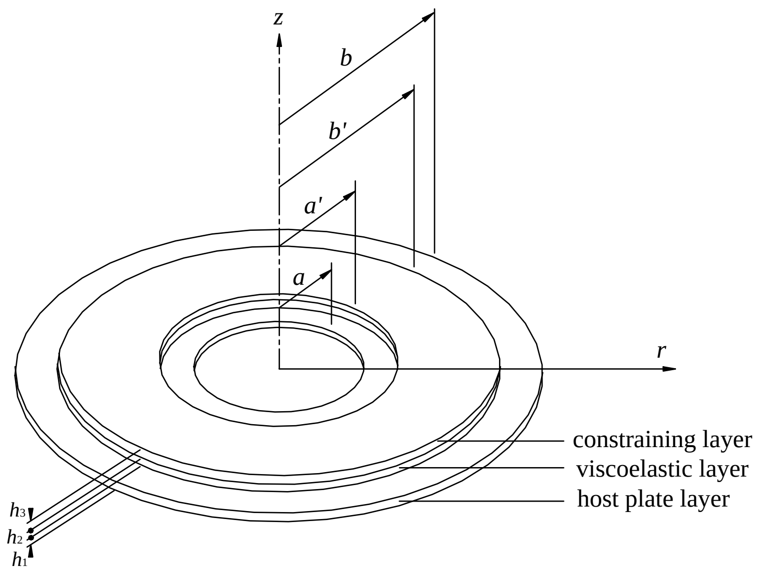

Fig. 1. Annular plate with partially constrained damping treatment.

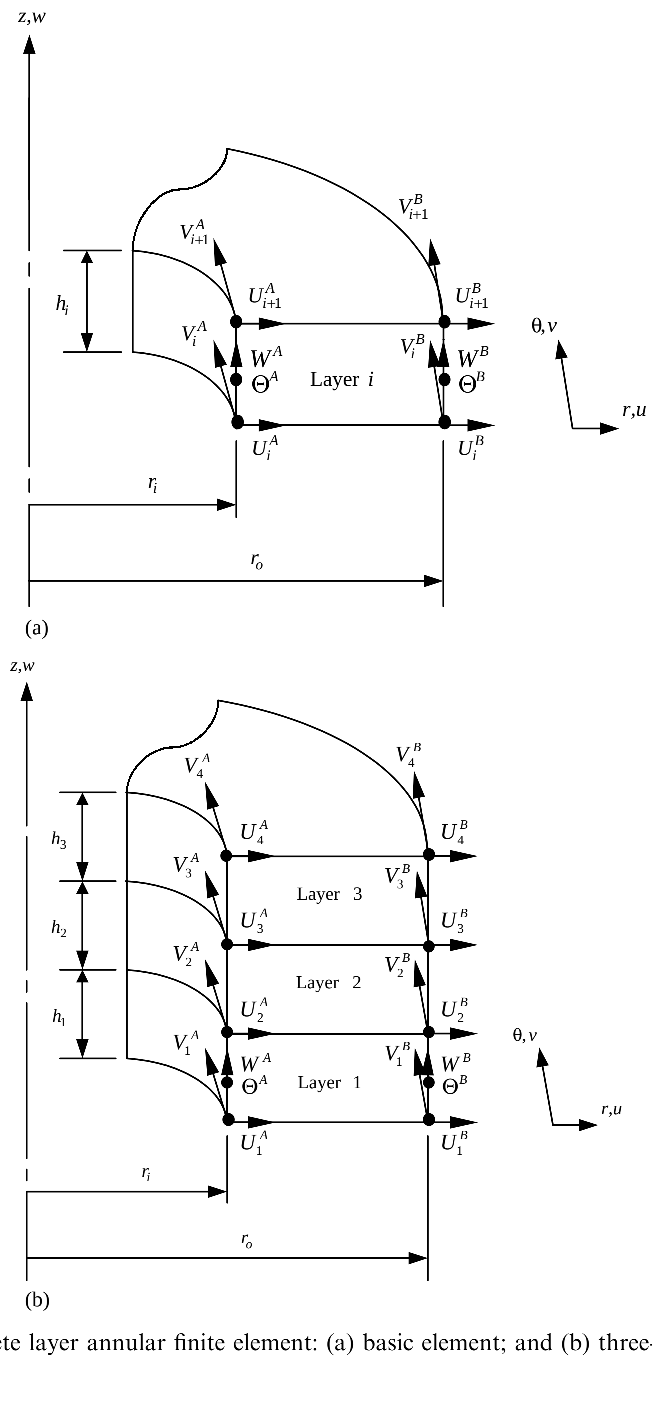

Fig. 2. Discrete layer annular finite element: (a) basic element; and (b) three-layer element.

where $\mathbf{L}_{1,i}$ is the transverse thickness interpolation matrix for layer i and is shown as

$$\mathbf{L}_{1,i}(z) = \begin{bmatrix} \left(\frac{1}{2}-\frac{z}{h_i}\right) & 0 & \left(\frac{1}{2}+\frac{z}{h_i}\right) & 0 & 0 \\ 0 & \left(\frac{1}{2}-\frac{z}{h_i}\right) & 0 & \left(\frac{1}{2}+\frac{z}{h_i}\right) & 0 \\ 0 & 0 & 0 & 0 & 1 \end{bmatrix}. \tag{2}$$

Using a further interpolation in the r direction and for the circumferential wave number m, the displacements of the two-layer interfaces can be expressed in terms of the nodal degrees of freedom:

$$\begin{Bmatrix} U_i(r,\theta,t) \\ V_i(r,\theta,t) \\ U_{i+1}(r,\theta,t) \\ V_{i+1}(r,\theta,t) \\ W(r,\theta,t) \end{Bmatrix} = \mathbf{L}_2(r,\theta)\mathbf{U}_i^e(t), \tag{3}$$

where $\mathbf{L}_2$, the interpolation matrix and $\mathbf{U}_i^e$, the vector of nodal displacements of the element, are given by

$$\mathbf{L}_2(r,\theta) = \begin{bmatrix} n_u^A & 0 & 0 & 0 & 0 & 0 & n_u^B & 0 & 0 & 0 & 0 & 0 \\ 0 & n_v^A & 0 & 0 & 0 & 0 & 0 & n_v^B & 0 & 0 & 0 & 0 \\ 0 & 0 & n_u^A & 0 & 0 & 0 & 0 & 0 & n_u^B & 0 & 0 & 0 \\ 0 & 0 & 0 & n_v^A & 0 & 0 & 0 & 0 & 0 & n_v^B & 0 & 0 \\ 0 & 0 & 0 & 0 & n_w^A & n_\Theta^A & 0 & 0 & 0 & 0 & n_w^B & n_\Theta^B \end{bmatrix}, \tag{4}$$

$$\mathbf{U}_i^e = \{\, U_i^A \quad V_i^A \quad U_{i+1}^A \quad V_{i+1}^A \quad W^A \quad \Theta^A \quad U_i^B \quad V_i^B \quad U_{i+1}^B \quad V_{i+1}^B \quad W^B \quad \Theta^B \}^{\mathrm{T}}, \tag{5}$$

$$n_u^A = (1-\xi)\cos m\theta, \quad n_u^B = \xi\cos m\theta, \quad n_v^A = (1-\xi)\sin m\theta, \tag{6a–c}$$

$$n_v^B = \xi\sin m\theta, \quad n_w^A = (1-3\xi^2+2\xi^3)\cos m\theta, \quad n_w^B = (3\xi^2-2\xi^3)\cos m\theta, \tag{6d–f}$$

$$n_\Theta^A = (\xi-2\xi^2+\xi^3)\cos m\theta, \quad n_\Theta^B = (-\xi^2+\xi^3)\cos m\theta, \quad \xi = \frac{r-r_i}{r_o-r_i}. \tag{6g–i}$$

The linear strains in the ith layer of the annular plate can be written in terms of the displacement

$$\boldsymbol{\varepsilon}_i = \mathscr{D}\mathbf{u}_i, \tag{7}$$

where the strain vector $\boldsymbol{\varepsilon}_i = \{\varepsilon_{r,i} \quad \varepsilon_{\theta,i} \quad \gamma_{r\theta,i} \quad \gamma_{rz,i} \quad \gamma_{\theta z,i}\}^{\mathrm{T}}$ and $\mathscr{D}$ is the differential operator matrix

$$\mathscr{D} = \begin{bmatrix} \dfrac{\partial}{\partial r} & 0 & 0 \\ \dfrac{1}{r} & \dfrac{1}{r}\dfrac{\partial}{\partial \theta} & 0 \\ \dfrac{1}{r}\dfrac{\partial}{\partial \theta} & \dfrac{\partial}{\partial r} - \dfrac{1}{r} & 0 \\ \dfrac{\partial}{\partial z} & 0 & \dfrac{\partial}{\partial r} \\ 0 & \dfrac{\partial}{\partial z} & \dfrac{1}{r}\dfrac{\partial}{\partial \theta} \end{bmatrix}. \tag{8}$$

The stress–strain relations for the ith layer can be expressed as

$$\begin{Bmatrix} \boldsymbol{\sigma}_{r,i} \\ \boldsymbol{\sigma}_{\theta,i} \\ \boldsymbol{\tau}_{r\theta,i} \\ \boldsymbol{\tau}_{rz,i} \\ \boldsymbol{\tau}_{\theta z,i} \end{Bmatrix} = \begin{bmatrix} C_{11,i} & C_{12,i} & 0 & 0 & 0 \\ C_{21,i} & C_{22,i} & 0 & 0 & 0 \\ 0 & 0 & C_{66,i} & 0 & 0 \\ 0 & 0 & 0 & C_{44,i} & 0 \\ 0 & 0 & 0 & 0 & C_{55,i} \end{bmatrix} \begin{Bmatrix} \varepsilon_{r,i} \\ \varepsilon_{\theta,i} \\ \gamma_{r\theta,i} \\ \gamma_{rz,i} \\ \gamma_{\theta z,i} \end{Bmatrix} \tag{9a}$$

or

$$\boldsymbol{\sigma}_i = \mathbf{C}_i \boldsymbol{\varepsilon}_i, \tag{9b}$$

where $\mathbf{C}_i$ is the elasticity matrix. For the isotropic material, the components of the elasticity matrix are

$$C_{11,i} = C_{22,i} = \frac{E_i}{1 - v_i^2}, \quad C_{12,i} = C_{21,i} = \frac{v_i E_i}{1 - v_i^2}, \tag{10a, b}$$

$$C_{44,i} = C_{55,i} = \kappa^2 \frac{E_i}{2(1 + v_i)}, \quad C_{66,i} = \frac{E_i}{2(1 + v_i)}, \tag{10c, d}$$

here E_i is Young's modulus, v_i is the Poisson ratio, and κ^2 is the shear correction factor. The shear correction factor is taken to be $\pi^2/12$ for layers 1 and 3, while to be 1 for layer 2. For the isotropic linear viscoelastic material, assuming that viscoelastic material is almost incompressible, the material constants are given by

$$E_i = E_v(1 + \mathrm{j}\eta_v), \quad v_i = 0.5 - \delta, \tag{11a, b}$$

where η_v is the loss factor of the viscoelastic material, δ is assumed to be a small constant real value (e.g., $\delta = 0.01$) which is introduced to avoid material stiffness singularities, and $\mathrm{j} = \sqrt{-1}$.

The kinetic and the strain energies of the element e of the ith layer can be written as

$$T_i^e = \frac{1}{2}\oint_{V_e} \rho_i \dot{\mathbf{u}}_i^{\mathrm{T}} \dot{\mathbf{u}}_i \, \mathrm{d}V, \tag{12}$$

$$U_i^e = \frac{1}{2}\oint_{V_e} \boldsymbol{\sigma}_i^{\mathrm{T}} \boldsymbol{\varepsilon}_i \, \mathrm{d}V, \tag{13}$$

where ρ_i is the mass density and $\oint_{V_e}$ represents a volume integral. Substituting Eqs. (1), (3), (7) and (9) into Eqs. (12) and (13), the kinetic and the strain energies can be arranged in the following forms:

$$T_i^e = \tfrac{1}{2}\dot{\mathbf{U}}_i^{e\mathrm{T}} \mathbf{M}_i^e \dot{\mathbf{U}}_i^e, \tag{14}$$

$$U_i^e = \tfrac{1}{2}\mathbf{U}_i^{e\mathrm{T}} \mathbf{K}_i^e \mathbf{U}_i^e, \tag{15}$$

where the elemental mass and stiffness matrices ($\mathbf{M}_i^e$ and $\mathbf{K}_i^e$) of the ith layer are

$$\mathbf{M}_i^e = \oint_{V_e} \rho_i (\mathbf{L}_{1,i}\mathbf{L}_2)^{\mathrm{T}} (\mathbf{L}_{1,i}\mathbf{L}_2) \, \mathrm{d}V, \tag{16}$$

$$\mathbf{K}_i^e = \oint_{V_e} (\mathscr{D}\mathbf{L}_{1,i}\mathbf{L}_2)^{\mathrm{T}} \mathbf{C}_i^{\mathrm{T}} (\mathscr{D}\mathbf{L}_{1,i}\mathbf{L}_2) \, \mathrm{d}V. \tag{17}$$

In order to combine the elemental matrices into the global mass and stiffness matrices, the transformation of element nodal co-ordinates to global co-ordinates must be obtained first, that is,

$$\mathbf{U}_i^e = \mathbf{T}_i^e \mathbf{U}, \tag{18}$$

where $\mathbf{U}$ is the global nodal co-ordinate vector and $\mathbf{T}_i^e$ is the transformation matrix. Hence, the global mass and stiffness matrices are assembled as

$$\mathbf{M} = \sum_{i=1}^{3} \left(\sum_{e=1}^{N_i} \mathbf{T}_i^{e\mathrm{T}} \mathbf{M}_i^e \mathbf{T}_i^e \right), \tag{19}$$

$$\mathbf{K} = \sum_{i=1}^{3} \left(\sum_{e=1}^{N_i} \mathbf{T}_i^{e\mathrm{T}} \mathbf{K}_i^e \mathbf{T}_i^e \right), \tag{20}$$

where N_i is the element number of the ith layer. And, the global equations of motion of the system can be formulated as

$$\mathbf{M}\ddot{\mathbf{U}} + \mathbf{K}\mathbf{U} = \mathbf{0}. \tag{21}$$

The boundary conditions are, for a clamped end

$$U = 0, \quad V = 0, \quad w = 0, \quad \Theta = 0, \tag{22a-d}$$

for a simply supported end

$$W = 0, \tag{23a}$$

$$U = 0, \quad V = 0, \quad \text{at an elemental corner on the edge.} \tag{23b}$$

In addition, the nodal displacements in the θ direction are all equal to zero ($V = 0$) for the axisymmertric vibration modes ($m = 0$).

Table 1
Non-dimensional natural frequencies of the annular plate made of single material ($a/b = 0.3$, $b/h = 10$,$v_1 = 0.3$)

	λ[a]									
	$N_r(N_z)$[b]	FF[c]	FS	FC	SF	SS	SC	CF	CS	CC
Mode (0,0)[d]	4(1)	4.98	2.81	6.78	2.06	12.46	19.79	4.06	18.10	27.20
	8(1)	4.98	2.80	6.75	2.06	12.29	19.03	3.98	16.96	24.68
	16(1)	4.98	2.80	6.74	2.06	12.25	18.84	3.95	16.68	24.09
	32(1)	4.98	2.80	6.73	2.06	12.24	18.79	3.95	16.61	23.92
	4(3)	5.00	2.81	6.78	2.06	12.42	19.66	4.05	17.98	26.94
	8(3)	4.98	2.80	6.74	2.06	12.26	18.91	3.96	16.85	24.45
	16(3)	4.98	2.80	6.72	2.06	12.21	18.72	3.95	16.57	23.85
	32(3)	4.97	2.80	6.72	2.06	12.20	18.67	3.94	16.50	23.69
	Irie [17]	4.98	2.80	6.73	2.06	12.24	18.77	3.95	16.57	23.85
	$N_r(N_z)$	FF	FS	FC	SF	SS	SC	CF	CS	CC
Mode (0,1)	4(1)	10.50	7.49	11.26	2.06	13.78	21.00	3.96	18.80	27.75
	8(1)	10.39	7.43	11.08	2.03	13.56	20.15	3.86	17.69	25.26
	16(1)	10.33	7.40	11.00	2.02	13.51	19.95	3.83	17.42	24.68
	32(1)	10.31	7.38	10.98	2.02	13.50	19.90	3.83	17.35	24.52
	4(3)	10.48	7.47	11.21	2.06	13.74	20.86	3.95	18.68	27.48
	8(3)	10.36	7.40	11.02	2.02	13.51	20.02	3.85	17.58	25.01
	16(3)	10.29	7.37	10.95	2.02	13.47	19.82	3.83	17.30	24.43
	32(3)	10.27	7.36	10.92	2.02	13.45	19.77	3.81	17.24	24.27
	Irie [17]	10.30	7.38	10.97	2.02	13.50	19.88	3.82	17.31	24.43

[a] Frequency parameter:, h = thickness of the plate.
[b] N_r = number of elements in the r direction, N_z = number of elements in the z direction.
[c] C = clamped, S = simply supported, F = free. The first letter denotes the edge condition at the inner edge.
[d] Mode (n, m): n = number of internal nodal circles, m = number of nodal diameters.

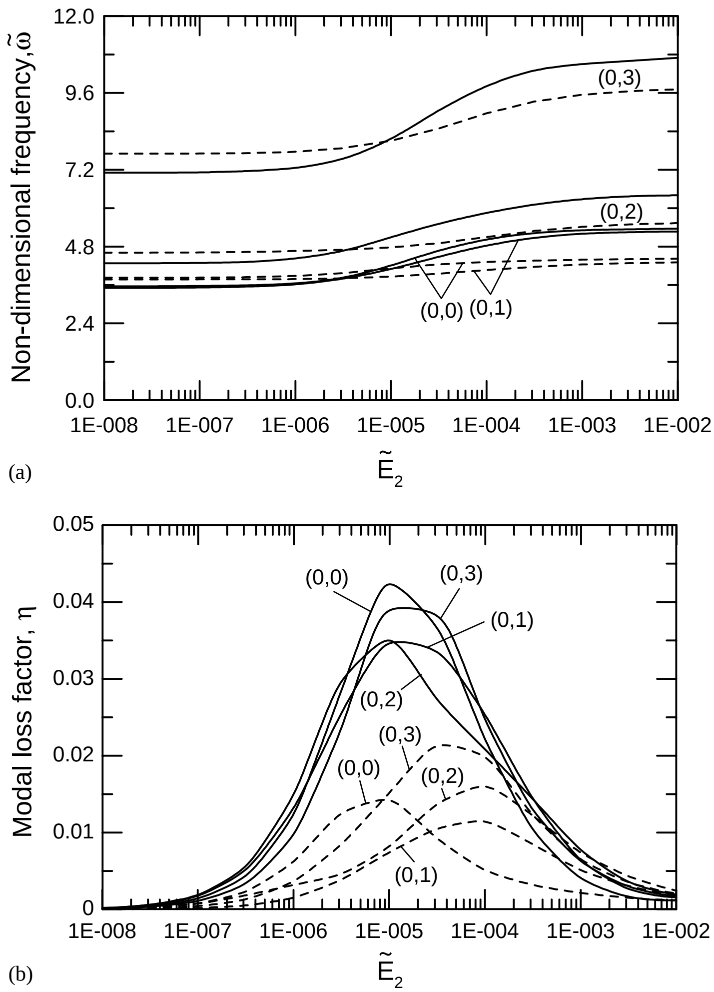

Fig. 3. Effects of $\tilde{E}_2$ on (a) the non-dimensional frequencies and (b) the modal loss factors of the plate. Key: ——, full treatment, $\tilde{a}' = 0.3$, and $\tilde{b}' = 1.0$; and - - - - -, partial treatment, $\tilde{a}' = 0.475$, and $\tilde{b}' = 0.825$ ($\tilde{\xi} = 0.3$, $\tilde{h}_2 = \tilde{h}_3 = 0.2$, $\tilde{b} = 200$, $\tilde{\rho}_2 = \tilde{\rho}_3 = 1$, $\tilde{E}_3 = 1$, $v_1 = v_3 = 0.3$, $\eta_v = 0.5$).

Complex eigenvalues $\tilde{\lambda}$ of the above complex eigenvalue problems can be found numerically, and both natural frequencies (ω) and modal loss factors (η) are extracted in the following manner [11]:

$$\omega = \sqrt{\mathrm{Re}(\tilde{\lambda})}, \quad \eta = \frac{\mathrm{Im}\,\tilde{\lambda}}{\mathrm{Re}(\tilde{\lambda})}. \tag{24a, b}$$

Note that the complex-valued terms of the stiffness matrix **K** in Eq. (21) are due to the strain energy terms of the viscoelastic material layer.

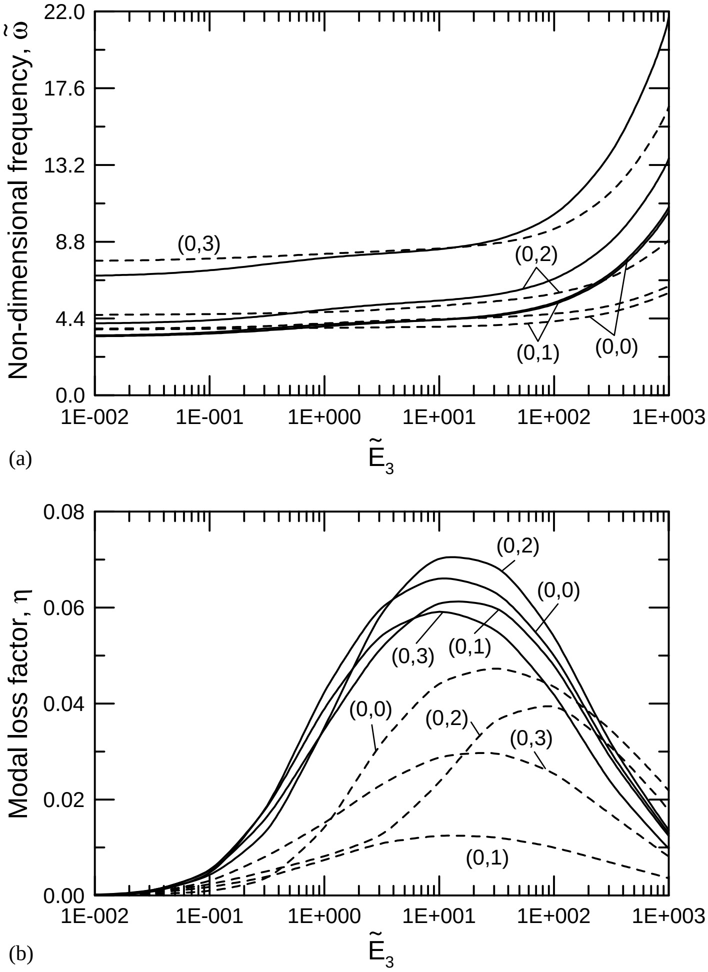

Fig. 4. Effects of $\tilde{E}_3$ on (a) the non-dimensional frequencies and (b) the modal loss factors of the plate. Key: ——, full treatment, $\tilde{a}' = 0.3$, and $\tilde{b}' = 1.0$; and -----, partial treatment, $\tilde{a}' = 0.475$, and $\tilde{b}' = 0.825$ ($\tilde{\xi} = 0.3$, $\tilde{h}_2 = \tilde{h}_3 = 0.2$, $\tilde{b} = 200$, $\tilde{\rho}_2 = \tilde{\rho}_3 = 1$, $\tilde{E}_2 = 10^{-5}$, $v_1 = v_3 = 0.3$, $\eta_v = 0.5$).

3. Numerical results and discussion

To verify the algorithm and calculations made in this paper, comparisons between the present results and results of existing simplify model [17] are made. The non-dimensional natural frequencies of single material thick annular plates are presented in Table 1. The material properties of plates are assumed to be linear elastic and isotropic, however, the one-layer and the three-layer elements in the thickness direction are both used in computation of natural frequencies. Good convergences and good agreements can be observed for both one-layer and three-layer element models. The number of elements in the *r* direction is taken to be 16 in the present studies and the viscoelastic material is introduced into layer 2.

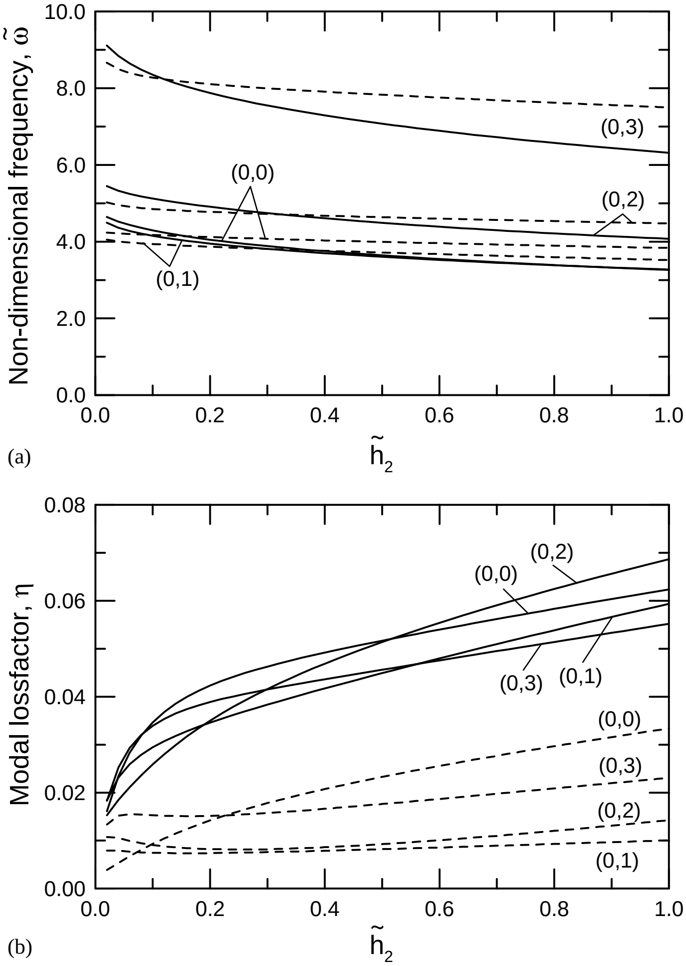

Fig. 5. Effects of $\tilde{h}_2$ on (a) the non-dimensional frequencies and (b) the modal loss factors of the plate. Key: ——, full treatment, $\tilde{a}' = 0.3$, and $\tilde{b}' = 1.0$; and -----, partial treatment, $\tilde{a}' = 0.475$, and $\tilde{b}' = 0.825$ ($\tilde{\xi} = 0.3$, $\tilde{h}_3 = 0.2$, $\tilde{b} = 200$, $\tilde{\rho}_2 = \tilde{\rho}_3 = 1$, $\tilde{E}_2 = 10^{-5}$, $\tilde{E}_3 = 1$, $v_1 = v_3 = 0.3$, $\eta_v = 0.5$).

For the sake of further analysis, the following non-dimensional parameters are introduced first:

$$\tilde{\xi} = \frac{a}{b}, \quad \tilde{a}' = \frac{a'}{b}, \quad \tilde{b}' = \frac{b'}{b}, \quad \tilde{b} = \frac{b}{h_1}, \quad \tilde{h}_2 = \frac{h_2}{h_1}, \quad \tilde{h}_3 = \frac{h_3}{h_1}, \quad \tilde{\rho}_2 = \frac{\rho_2}{\rho_1}, \tag{25a−g}$$

$$\tilde{\rho}_3 = \frac{\rho_3}{\rho_1}, \quad \tilde{E}_2 = \frac{\mathrm{Re}(E_2)}{E_1}, \quad \tilde{E}_3 = \frac{E_3}{E_1}, \quad \tilde{\omega} = \frac{2b^2\omega}{h_1}\sqrt{\frac{\rho_1}{E_1}}. \tag{25h−k}$$

The non-dimensional frequencies and modal loss factors of plates with constrained damping treatments are given in Figs. 3(a) and (b). The effects of the modulus of viscoelastic layer $\tilde{E}_2$ are studied. The boundary conditions of the annular plate are taken to be clamped at inner radius and

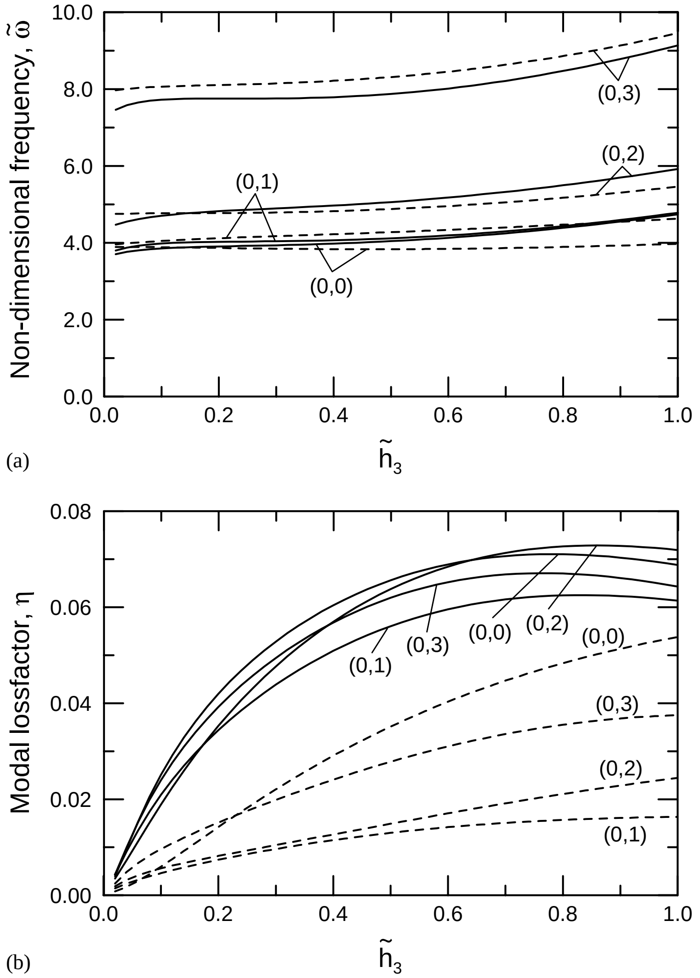

Fig. 6. The effects of $\tilde{h}_3$ on (a) the non-dimensional frequencies and (b) the modal loss factors of the plate. Key: ——, full treatment, $\tilde{a}' = 0.3$, $\tilde{b}' = 1.0$; and -----, partial treatment, $\tilde{a}' = 0.475$, and $\tilde{b}' = 0.825$ ($\tilde{\xi} = 0.3$, $\tilde{h}_2 = 0.2$, $\tilde{b} = 200$, $\tilde{\rho}_2 = \tilde{\rho}_3 = 1$, $\tilde{E}_2 = 10^{-5}$, $\tilde{E}_3 = 1$, $v_1 = v_3 = 0.3$, $\eta_v = 0.5$).

free at outer radius. In order to cover a wide range of $\tilde{E}_2$, a logarithmic scale has been used. Both the cases of fully and partially constrained damping treatment are solved for different modes (n, m). It can be observed that the modulus $\tilde{E}_2$ has significant influences on both non-dimensional frequencies and modal loss factors. It is shown that the plates with full treatment have lower natural frequencies than those with partial treatment at the lower values of $\tilde{E}_2$, but the reverse effects can be seen at the higher values of $\tilde{E}_2$. It is implied that the contribution of $\tilde{E}_2$ to the stiffness of the plates with full treatment is more obvious than those with partial treatment as $\tilde{E}_2$ increases. As for the modal loss factors, it can be seen that the modal loss factors increase with increasing of $\tilde{E}_2$ at the lower value of $\tilde{E}_2$, but as $\tilde{E}_2$ increases above a certain value, the phenomenon is reversed. These are similar to those reported in a rectangular composite plate with

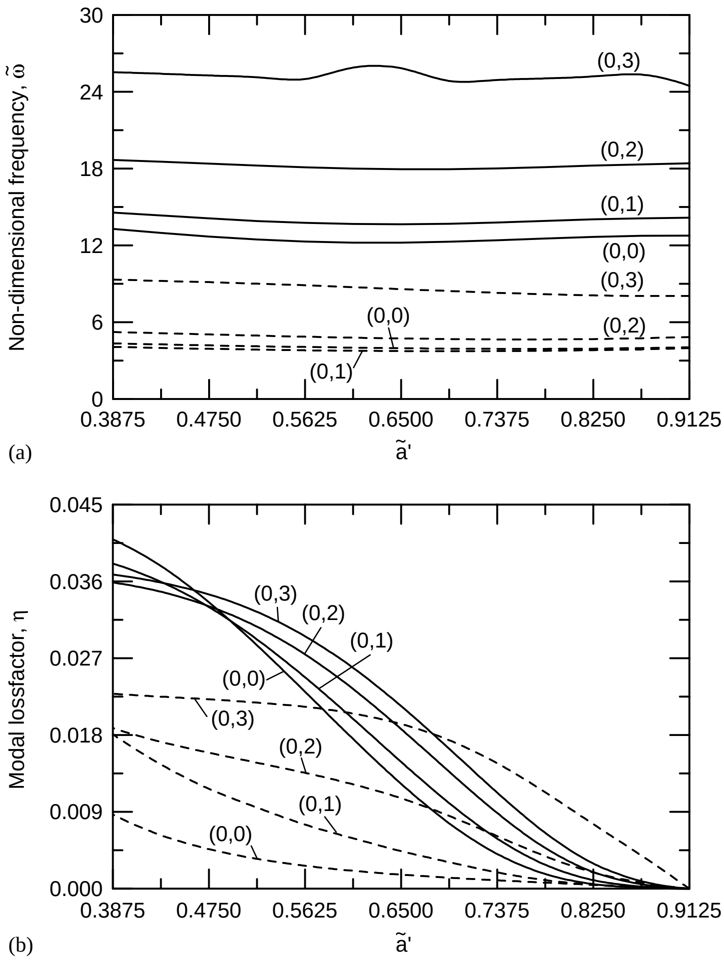

Fig. 7. Effects of $\tilde{a}'$ with different boundary conditions. Key: ——, simply–simply supported; and - - - - -, clamped–free ($\tilde{\xi} = 0.3$, $\tilde{h}_2 = \tilde{h}_3 = 0.2$, $\tilde{b} = 200$, $\tilde{b}' = 0.9125$, $\tilde{\rho}_2 = \tilde{\rho}_3 = 1$, $\tilde{E}_2 = 10^{-4}$, $\tilde{E}_3 = 1$, $v_1 = v_3 = 0.3$, $\eta_v = 0.5$).

a viscoelastic mid-layer [12]. It is also shown roughly that the plates with full treatment have better damping properties than the plates with partial treatment in this case.

The effects of the modulus of the constraining layer $\tilde{E}_3$ on the non-dimensional frequencies and modal loss factors are sketched in Figs. 4(a) and (b). It is shown that the modulus $\tilde{E}_3$ also has significant effects on the non-dimensional frequencies and modal loss factors. As expected, the non-dimensional frequencies increase when the modulus $\tilde{E}_3$ becomes larger. It is also shown that the effects of the modulus $\tilde{E}_3$ on modal loss factors are similar to the effects of the modulus $\tilde{E}_2$.

The effects of the thickness of the viscoelastic material layer and the constraining layer on the non-dimensional frequencies and modal loss factors are now considered. The effects of $\tilde{h}_2$ on non-dimensional frequencies and modal loss factors are shown in Figs. 5(a) and (b). Because the additional constraining and damping layers are always thinner than the host plate in practice, the

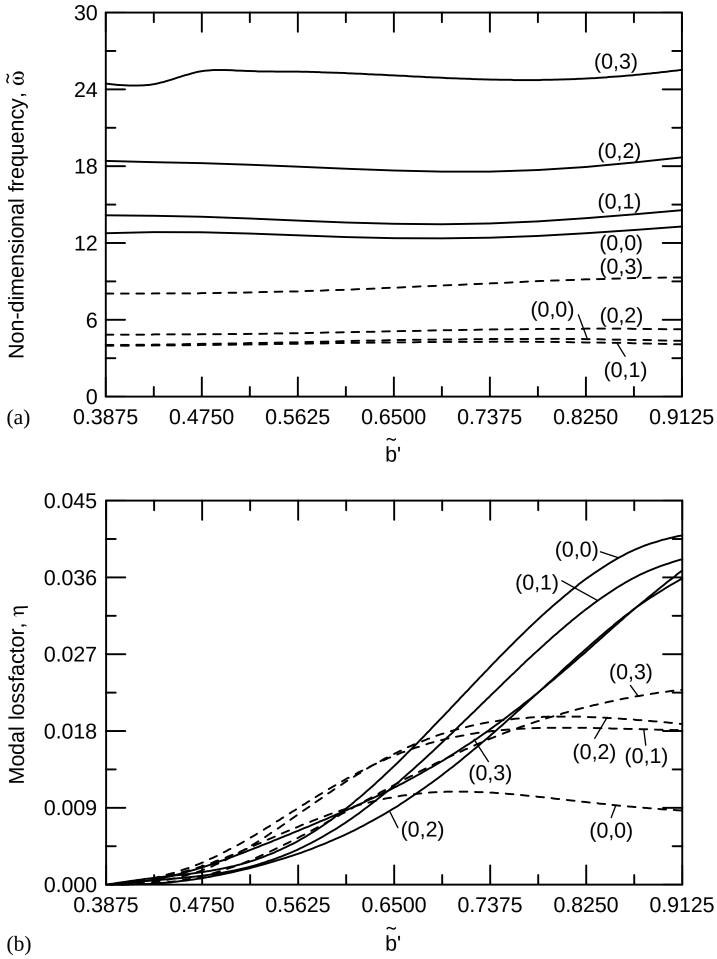

Fig. 8. Effects of $\tilde{b}'$ with different boundary conditions. Key: ——, simply–simply supported; and - - - - -, clamped–free ($\tilde{\xi} = 0.3$, $\tilde{h}_2 = \tilde{h}_3 = 0.2$, $\tilde{b} = 200$, $\tilde{a}' = 0.3875$, $\tilde{\rho}_2 = \tilde{\rho}_3 = 1$, $\tilde{E}_2 = 10^{-4}$, $\tilde{E}_3 = 1$, $\nu_1 = \nu_3 = 0.3$, $\eta_v = 0.5$).

non-dimensional thickness parameter $\tilde{h}_2$ is plotted in the range less than one. The comparisons of the plates with fully and partially constrained damping treatments are made again. It can be seen that the frequencies decrease as $\tilde{h}_2$ increases. The reason is that the contribution of the increase of thickness of the viscoelastic layer to the stiffness matrix of the composite plates is more insignificant than those to the mass matrix of the plates. It can be observed that the modal loss factors always increase as $\tilde{h}_2$ increases for the full treatment plates, but it is not the case for the partial ones. The phenomenon is related to the stiffness of the three layers and will be mentioned later. The effects of $\tilde{h}_3$ on non-dimensional frequencies and modal loss factors are plotted in Figs. 6(a) and (b). It can be found that the frequencies increase as $\tilde{h}_3$ increases. It is because the stiffness of the plates increases with increasing of the thickness of the constraining layer. It also can be seen that the modal loss factors climb to a maximum value at an optimum value in the case of fully

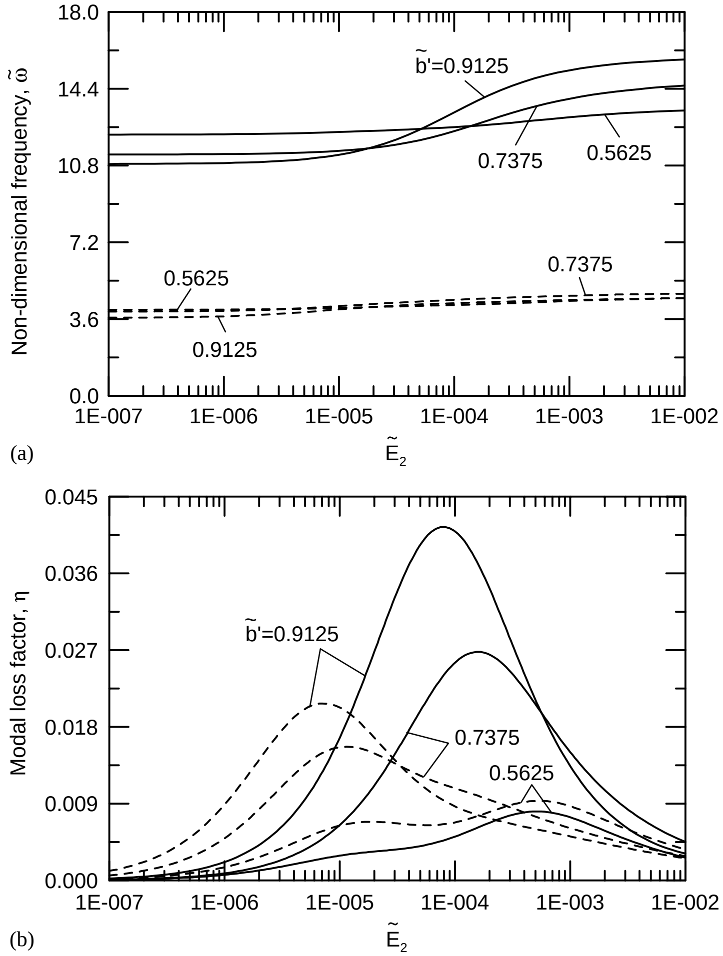

Fig. 9. The effects of $\tilde{b}'$. Key: ——, simply–simply supported; and - - - - -, clamped–free ($\tilde{\xi} = 0.3$, $\tilde{h}_2 = \tilde{h}_3 = 0.2$, $\tilde{b} = 200$, $\tilde{a}' = 0.3875$, $\tilde{\rho}_2 = \tilde{\rho}_3 = 1$, $\tilde{E}_3 = 1$, $\nu_1 = \nu_3 = 0.3$, $\eta_v = 0.5$).

covered plate, but the maximum modal loss factor for the partially covered plate is not shown when $\tilde{h}_3$ less than one.

The effects of treatment size of the plates with different boundary conditions are presented in Figs. 7 and 8. The case of the outer radius of the constrained damping treatment $\tilde{b}'$ being fixed while the inner radius $\tilde{a}'$ is varied is illustrated in Fig. 7. The modal loss factors decrease as the inner radius $\tilde{a}'$ increases, that is, the modal loss factors decrease as the treatment size decreases. The case of the inner radius $\tilde{a}'$ being fixed while the outer radius $\tilde{b}'$ is varied is shown in Fig. 8. It can be seen that the modal loss factors of the plate with clamped–free boundaries are smaller than those of the plate with simply supported boundaries when the values of $\tilde{b}'$ are large. It is seen that the modal loss factors do not always increase when the treatment coverage increases. This is related to the stiffness of the layers and is illustrated in Fig. 9 which shows the effects of $\tilde{b}'$ on the

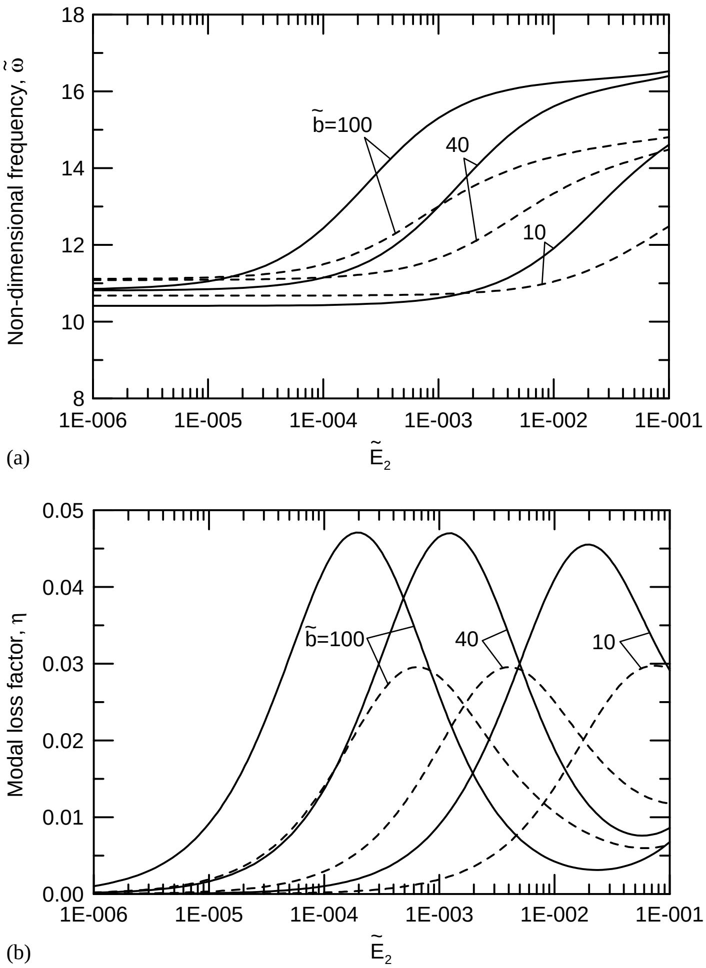

Fig. 10. The effects of $\tilde{b}$. Key: ——, full treatment, $\tilde{a}' = 0.3$, $\tilde{b}' = 1.0$; and - - - - -, partial treatment, $\tilde{a}' = 0.475$, and $\tilde{b}' = 0.825$ (Boundary condition: simply–simply supported, $\tilde{\xi} = 0.3$, $\tilde{h}_2 = \tilde{h}_3 = 0.2$, $\tilde{\rho}_2 = \tilde{\rho}_3 = 1$, $\tilde{E}_3 = 1$, $v_1 = v_3 = 0.3$, $\eta_v = 0.5$).

non-dimensional frequencies and modal loss factors of the mode (0,0). The non-dimensional inner radius of the treatment $\tilde{a}'$ is taken to be 0.3875, and the outer radius of the treatment $\tilde{b}'$ is chosen to be 0.5625, 0.7375, and 0.9125, respectively. It can be seen that the modal loss factors increase as the treatment size increases at the smaller value of $\tilde{E}_2$, but the reverse effect can be seen at some larger value of $\tilde{E}_2$.

Finally, the effects of the ratio of the outer radius to thickness of the host plate $\tilde{b}$ are considered in Fig. 10. It is shown that the transition regions of the frequencies are shifted to right as the plates become thicker, and the modal loss factor curves are shifted in the same way. It implies that a larger value of stiffness of the viscoelastic layer $\tilde{E}_2$ has to be chosen to achieve a higher damping for a thicker host plate. The results are also similar to those of a three-layered rectangular plate with a viscoelastic mid-layer presented by Cupial and Niziol [12].

4. Conclusions

The paper presents the vibration and damping characteristics of the annular plate with constrained damping treatment. By using the discrete layer annular finite element and the complex description of the viscoelastic material, the natural frequencies and modal loss factors of the partially or fully damping treatment are obtained easily. Numerical results show that the thickness and stiffness of the constrained damping layer and the size of the treatment have significant effects on the natural frequencies and modal loss factors of the plate. It is also found that the damping properties of the plate with the full treatment are not always larger than those with the partial treatment. The relative stiffness and thickness of the constraining layer, the damping layer, and the host plate must be taken into account when the damped annular plate is designed to achieve a high damping characteristic.

Appendix A. Nomenclature

a	inner radius of the host plate
a'	inner radius of the treatment
$\tilde{a}'$	a'/b, non-dimensional inner radius of the treatment
b	outer radius of the host plate
b'	outer radius of the treatment
$\tilde{b}$	b/h_1, outer radius-to-thickness ratio of the host plate
$\tilde{b}'$	b'/b, non-dimensional outer radius of the treatment
E_i	Young's modulus of the ith layer
E_v	stiffness of the viscoelastic material
$\tilde{E}_2$	$\mathrm{Re}(E_2)/E_1$, non-dimensional stiffness of layer 2
$\tilde{E}_3$	E_3/E_1 , non-dimensional stiffness of layer 3
h	thickness of the host plate
h_i	thickness of the ith layer
$\tilde{h}_2$	h_2/h_1, non-dimensional thickness of layer 2
$\tilde{h}_3$	h_3/h_1, non-dimensional thickness of layer 3
i	index for layer, $i = 1, 2, 3$
m	circumferential wave number
n	number of internal nodal circles
N_r	number of elements in the r direction
N_z	number of elements in the z direction
η	modal loss factor of the composite plate
η_v	loss factor of the viscoelastic material
λ	frequency parameter
v_i	the Poisson ratio of the ith layer
$\tilde{\xi}$	a/b, non-dimensional inner radius of the host plate
ρ_i	mass density of the ith layer
$\tilde{\rho}_2$	ρ_2/ρ_1, non-dimensional mass density of layer 2
$\tilde{\rho}_3$	ρ_3/ρ_1, non-dimensional mass density of layer 3
ω	natural frequency
$\tilde{\omega}$	$(2b^2\omega/h_1)\sqrt{\rho_1/E_1}$, non-dimensional frequency

References

[1] D. Nashif, D.I.G. Jones, J.P. Henderson, Vibration Damping, Wiley, New York, 1985.

[2] D.J. Mead, The effect of certain damping treatments on the responses of idealized aeroplane structures excited by noise, Air Force Materials Laboratory Report AFML-TR-65-284, WPAFB, 1965.

[3] E.M. Kerwin Jr., Damping of flexural waves by a constrained viscoelastic layer, Journal of the Acoustical Society of America 31 (1959) 952–962.

[4] D. Ross, E.E. Ungar, E.M. Kerwin Jr., Damping of plate flexural vibrations by means of viscoelastic laminate, in: Structure Damping, ASME, New York, 1959, Section 3, pp. 48–88.

[5] R.A. DiTaranto, Theory of vibratory bending for elastic and viscoelastic layered finite-length beams, American Society Mechanical Engineers Journal of Applied Mechanics 32 (1965) 881–886.

[6] D.J. Mead, S. Markus, The forced vibrations of a three-layer damped sandwich beam with arbitrary boundary conditions, American Institute of Aeronautics and Astronautics Journal 10 (1969) 163–175.

[7] D.J. Mead, The damping properties of elastically supported sandwich plates, Journal of Sound and Vibration 24 (1972) 275–295.

[8] Y.V.K.S. Rao, B.C. Nakra, Vibrations of unsymmetrical sandwich beams and plates with viscoelastic cores, Journal of Sound and Vibration 34 (1974) 309–326.

[9] J.F. He, B.A. Ma, Analysis of flexural vibration of viscoelastically damped sandwich plates, Journal of Sound and Vibration 126 (1988) 37–47.

[10] D.K. Rao, Vibration of short sandwich beams, Journal of Sound and Vibration 52 (1977) 253–263.

[11] R. Rikards, A. Chate, E. Barkanov, Finite element analysis of damping the vibrations of laminated composites, Computers and Structures 47 (1993) 1005–1015.

[12] P. Cupial, J. Niziol, Vibration and damping analysis of a three-layered composite plate with a viscoelastic mid-layer, Journal of Sound and Vibration 183 (1995) 99–114.

[13] J.A. Zapfe, G.A. Lesieutre, A discrete layer beam finite element for the dynamic analysis of composite sandwich beams with integral damping layers, Computers and Structures 70 (1999) 647–666.

[14] S. Mirza, A.V. Singh, Axisymmetric vibration of circular sandwich plates, American Institute of Aeronautics and Astronautics Journal 12 (1974) 1418–1420.

[15] P.K. Roy, N. Ganesan, A vibration and damping analysis of circular plates with constrained damping layer treatment, Computers and Structures 49 (1993) 269–274.

[16] S.C. Yu, S.C. Huang, Vibration of a three-layered viscoelastic sandwich circular plate, International Journal of Mechanical Sciences 43 (2001) 2215–2236.

[17] T. Irie, G. Yamada, K. Takagi, Natural frequencies of thick annular plates, Journal of Applied Mechanics 49 (1982) 633–638.